

# Effects of Three-Dimensional Bedrock Topography on Earthquake Motions in Sedimentary Basins

ARTHUR FRANKEL

Work being done at the U.S. Geological Survey on 3-D simulations of earthquake ground motions in sedimentary basins is described. The ultimate goal of this research is to predict strong ground motions in sedimentary basins for expected large earthquakes. Throughout this paper, the inadequacy of using flat-layered models for synthesizing ground motions in sedimentary basins is emphasized. It has been demonstrated with 2-D and 3-D simulations how the slope of the alluvium-bedrock interface can trap S-waves in the basins, producing prolonged trains of surface waves. These surface waves are not generated in flat-layered models, which underestimate the duration and peak amplitude of shaking. It is necessary to account for the increased duration and amplitude of surface waves in sedimentary basins when designing man-made structures with natural periods of 1 sec and greater. Results are presented for 3-D simulations of earthquakes on the San Andreas fault in the San Bernardino and Santa Clara valleys in California. These simulations show the importance of S-wave-to-surface-wave conversions at the edges of the valleys. A contour map of maximum ground velocity in the San Bernardino Valley is produced from the simulation of a magnitude 6.5 earthquake on the San Andreas fault. Areas of especially large ground motions occur where surface waves reflected from the edges of the basin constructively interfere with trapped waves behind the direct S-wave.

The estimation of ground motions in sedimentary basins is crucial for the design of earthquake-resistant structures. It is common practice to assume a horizontal interface between the alluvium and bedrock when ground motions for alluvial sites are calculated. However, many observational and theoretical studies have demonstrated the inadequacy of using flat-layered models to predict ground motions for sites in sedimentary basins (1-3). Figure 1 shows schematically the wave types affecting a site in an alluvial basin. The direct S-wave will be amplified by the alluvium and is shown as the ray path that is steeply incident below the basin site. There will also be multiple reflections of the S-wave in the alluvium. In addition, the direct S-wave will convert to a trapped surface wave at the margin of the basin because of the dip of the alluvium-bedrock interface. Theoretical studies using 2-D models have demonstrated the importance of this S-wave-to-surface-wave conversion (1). In these theoretical studies, the converted surface wave can be the largest phase in the synthetic seismogram at periods of 1 sec and greater and, because of its slow group velocity, can vastly prolong the duration of

shaking. Such converted surface waves have been observed in recordings of the 1971 San Fernando earthquake (2) and aftershocks of the 1989 Loma Prieta earthquake (3). It has been suggested that the prolonged, damaging ground motions in Mexico City from the 1985 Michoacan earthquake were composed of such surface waves (4).

Obviously, the presence of these large surface waves has profound implications on the design of structures with natural periods of 1 sec and longer. Models with horizontal layering do not predict these S-wave-to-surface-wave conversions, which can be much larger than the amplitude of the surface waves generated at the source.

Some observational studies have demonstrated that these surface waves can be reflected along various edges of an alluvial basin, highlighting the need for 3-D simulations to predict ground motions accurately. For example, observations of Loma Prieta aftershocks using a dense array in Sunnyvale showed that much of the longer-period ( $f \leq 1$  Hz) energy after the S-wave is composed of surface waves, some of which come from azimuths very different from the source (3). Surface waves scattered from specific locations near the edges of alluvial basins were reported by Phillips et al. (5) and Spudich and Iida (6) for the Kanto Basin in Japan and the Coachella Valley in California, respectively.

This paper documents the results from 3-D numerical simulations of ground motions in the San Bernardino and Santa Clara valleys in southern and northern California, respectively, during earthquakes on the San Andreas fault. Each of these areas is a major population center containing many large structures that are vulnerable to seismic shaking at periods of 1 sec and larger. Thus, understanding the propagation of surface waves in these valleys is critical to designing earthquake-resistant structures.

## METHOD

The finite-difference method was used to propagate the complete elastic wavefield through 3-D models of sedimentary basins. The wavefield includes P, SH, and SV waves, converted phases, surface waves, multiple reflections, diffractions, and head waves. The method has been described in more detail by Frankel and Vidale (7). Let  $u$ ,  $v$ , and  $w$  be the displacements in the  $x$ ,  $y$ , and  $z$  directions, respectively.  $\rho$  denotes density and  $\lambda$  and  $\mu$  are the Lamé constants. These medium properties vary with position. The three coupled wave

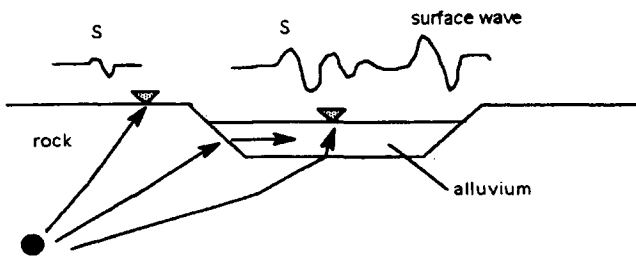


**FIGURE 1** Schematic vertical cross section of ray paths between the hypocenter (*solid circle*) and sites on rock and in an alluvial basin (*inverted triangles*). Idealized seismograms for the rock and alluvial sites are shown above each receiver. The surface wave at the alluvial site is produced by conversion of the S-wave at the left edge of the basin.

equations are

$$\begin{aligned} \rho u_{tt} &= [(\lambda + 2\mu)u_x + \lambda w_z + \lambda v_y]_x \\ &\quad + (\mu u_y + \mu v_x)_y + (\mu u_z + \mu w_x)_z \\ \rho v_{tt} &= [(\lambda + 2\mu)v_y + \lambda w_z + \lambda u_x]_y \\ &\quad + (\mu v_x + \mu u_y)_x + (\mu v_z + \mu w_y)_z \\ \rho w_{tt} &= [(\lambda + 2\mu)w_z + \lambda u_x + \lambda v_y]_z \\ &\quad + (\mu w_x + \mu u_z)_x + (\mu w_y + \mu v_z)_y \end{aligned} \quad (1)$$

Here subscripts denote partial derivatives. The model of the sedimentary basin can be arbitrarily complicated.

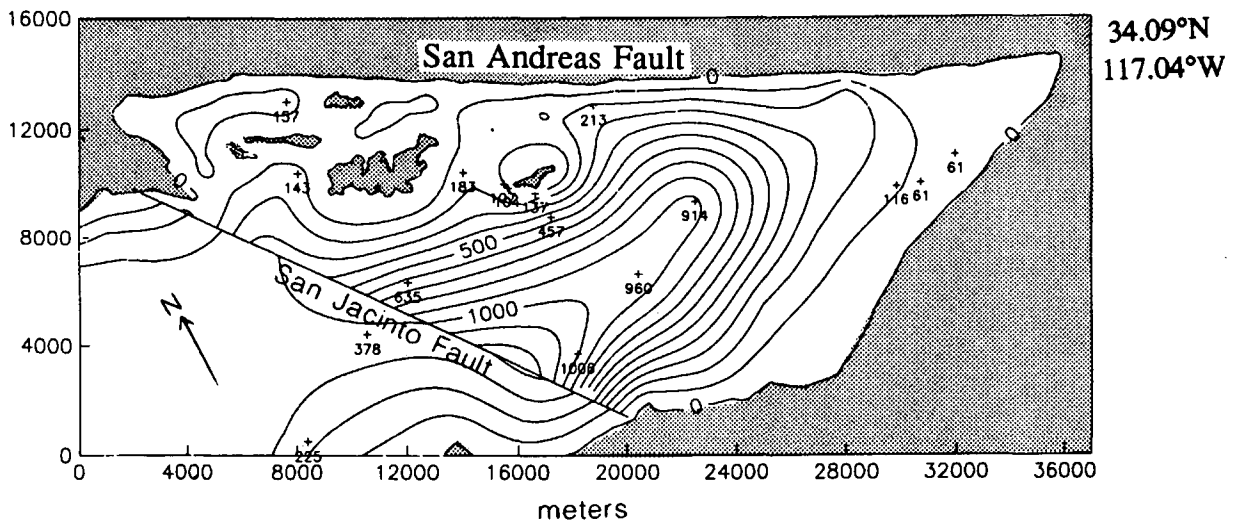
In the simulations described below, a grid spacing of 100 m was used. Given this grid spacing and the slowest S-wave velocity in the grid (0.6 km/sec), the simulations are accurate up to 1 Hz. Each grid contained about 4 million grid points.

The simulations described here were performed on a Cray YMP supercomputer. A run of 5,000 time steps takes about 8 CPU-hr on the Cray. Since each time step corresponds to 0.012 sec, such a run simulates 60 sec of ground motion. Videotapes have been made of the simulations described in this paper.

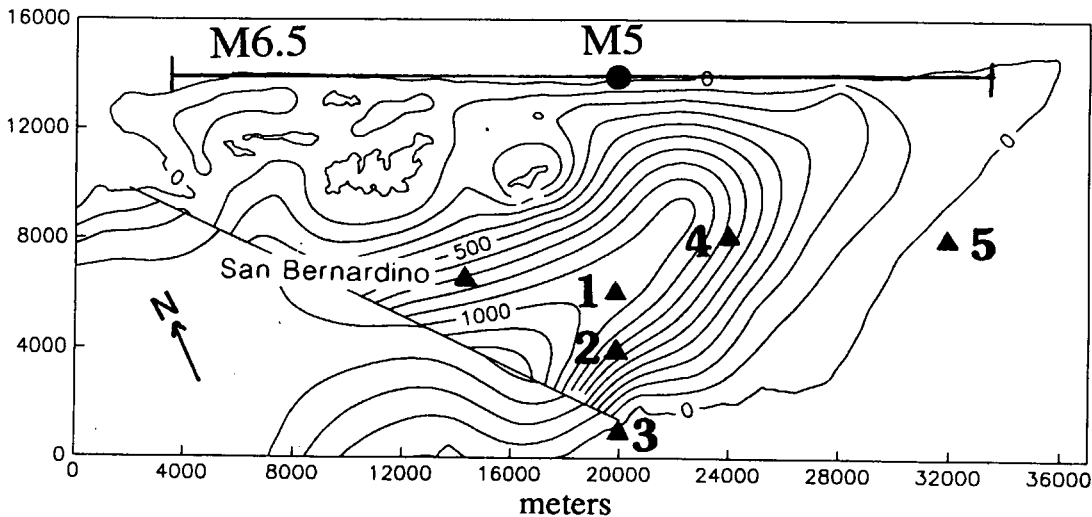
## SAN BERNARDINO VALLEY SIMULATIONS

Figure 2 shows the area of the simulations for the San Bernardino Valley in southern California. These simulations are described in more detail by Frankel (8). The 3-D grid corresponds to 37 by 16 by 7 km in depth. The basin model was derived from the limited water well and oilwell data available, as well as one refraction line. For the alluvium, the shear wave velocity used was 0.6 km/sec; the P-wave velocity, 1.1 km/sec; and the density, 2.0 g/cc. For the rock just below the alluvium, the shear wave velocity used was 2.0 km/sec; the P-wave velocity, 3.5 km/sec; and the density, 2.6 g/cc. Below 3 km depth,  $V_p$  increased to 5.0 km/sec and  $V_s$  increased to 2.9 km/sec. Two hypothetical earthquakes along the San Andreas fault were considered: a moment-magnitude (M) 5 (point source, 6 km depth) and an M6.5 earthquake that ruptured a 30-km-long segment of the fault (Figure 3). The M6.5 earthquake ruptured from northwest to southeast along the fault at a rupture velocity of  $0.8V_s$ , with slip occurring over a depth range of 3.5 to 6.5 km. For both events, the slip velocity at any point on the fault was a truncated Gaussian pulse with a width of 1.0 sec. Both earthquakes were pure strike slip on vertical fault. A filtered random number field was used to represent slip on the fault. The realization used here had large areas of slip (asperities) near both ends of the fault.

The difference between synthetics from the 3-D simulation and those from a flat-layered (1-D) model is dramatic (Figure 4, for M5). The 3-D simulation has a much longer duration of shaking than the 1-D model. The basic reason for this is



**FIGURE 2** Map of San Bernardino Valley with outcrops of bedrock shaded. Crosses indicate depth to basement (in meters) from wells and from one refraction line; 635-m value is conjecture. Contours show depth to basement (in meters) used in simulation (100-m contour interval). Grid size was 370 by 160 by 70 (depth), with a grid spacing of 100 m.



**FIGURE 3** Location of moment magnitude M5 (circle) and M6.5 earthquakes along the San Andreas fault that were used in the simulations. The earthquakes were specified using their equivalent double couples in the grid. Triangles show receivers with displayed synthetics. Contour interval is 100 m.

the trapping of body waves in the alluvium that occurs in the 3-D simulation. The incident S-wave is essentially converted into surface waves (Rayleigh and Love) at the margins of the basin. These surface waves have relatively slow group velocities and prolong the duration of shaking in the basin. Models using flat layers cannot account for these body-wave-to-surface-wave conversions. The 2-D simulation shows some of the surface waves but considerably underestimates the duration of shaking compared with the 3-D simulation. The 3-D sim-

ulation contains substantial surface wave energy coming from azimuths different from the source direction, energy not modeled by the 2-D simulation.

Figure 5 contains the ground velocity from the 3-D simulation for the San Bernardino site for the M6.5 earthquake. The 3-D simulations do not include anelastic attenuation, which is incorporated into the sediments by convolving the synthetics with a time-varying  $Q$ -operator. The bottom seismograms in Figure 5 show the result for a shear wave  $Q$  of

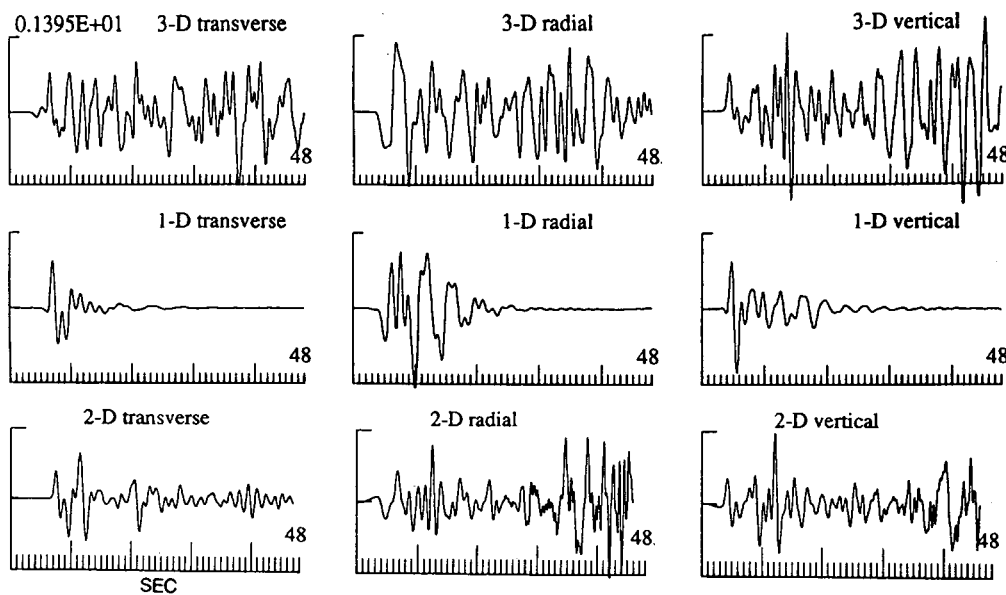


**FIGURE 4** *Top:* Velocity synthetics from 3-D simulation of M5 event for San Bernardino site. *Middle:* Reflectivity synthetics for same site using flat-layered model. *Bottom:* Synthetics from 2-D finite-difference simulation (vertical cross section). Note large duration of synthetics from 3-D model compared with those from 1-D model. All synthetics are plotted with same scale. Peak amplitude is given in centimeters per second; time scale is marked in seconds.

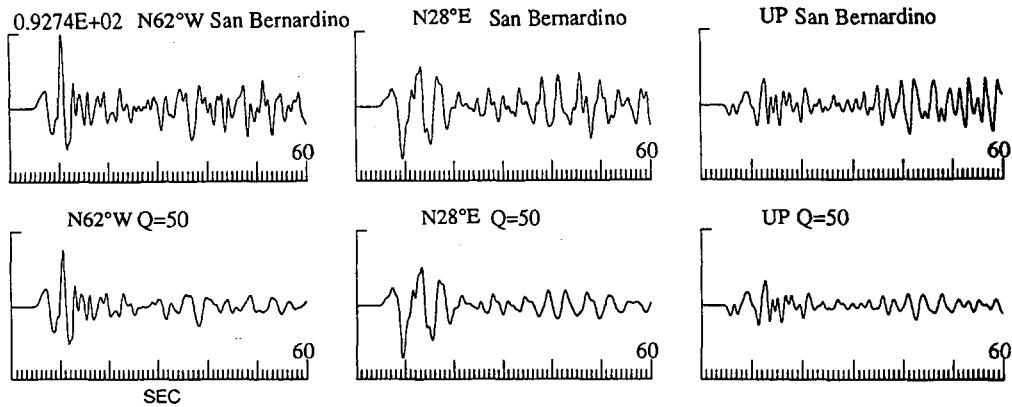


**FIGURE 5** Velocity synthetics at San Bernardino from 3-D simulation of M6.5 earthquake (*top*) with no anelastic attenuation and (*bottom*) using  $Q$  of 50 in alluvium. Peak amplitude is given in centimeters per second. Synthetics are plotted with the same scale. Seismograms are for horizontal motion parallel to the fault strike (*left*, N62°W), horizontal motion perpendicular to the fault strike (*middle*, N28°E), and vertical motion (*right*).

50 in the sediments. High-frequency energy is significantly reduced in the later part of the synthetics. The substantial differences between shaking at basin and rock sites are shown in Figures 6 and 7, which give the synthetic seismograms at nearby rock and alluvium sites. Peak-to-peak amplitudes are three to seven times larger for the basin sites than the rock sites in these examples. The duration of shaking is much longer for the basin sites than the rock sites, primarily because of trapped waves in the sediment. The top set of seismograms in Figure 7 shows the largest peak velocities found in the simulation (Site 4). These large velocities are caused by a number of factors: directivity of the source, constructive interference from rupture events at different parts of the fault, and constructive interference of trapped waves generated along the near and far edges of the basin. Figure 8 is a contour plot of the maximum horizontal velocities from the 3-D simulation. In general, basin sites exhibit much larger peak velocities than the rock sites. The largest velocities occur near the deepest part of the basin. The location of the largest ground motions

is dependent on the rupture direction, asperity positions, and radiation pattern of the earthquake.

#### SANTA CLARA VALLEY SIMULATION

Ground motions were also simulated for an  $M_L$  4.4 aftershock of the Loma Prieta earthquake. This aftershock was recorded by a dense array of four seismometers at Sunnyvale in the Santa Clara Valley (Figure 9). The 3-D simulation covered the area of the Santa Clara Valley shown in Figure 10 (30 by 22 by 6 km in depth, 100-m grid spacing). The alluvium and rock properties used in this simulation were the same as those in the San Bernardino simulation but did not include the higher velocities below 3 km. The results of the Santa Clara Valley simulation have been discussed in detail by Frankel and Vidale (7).

Synthetic seismograms along a north-south profile are shown in Figure 11. Note the large difference in amplitude and du-

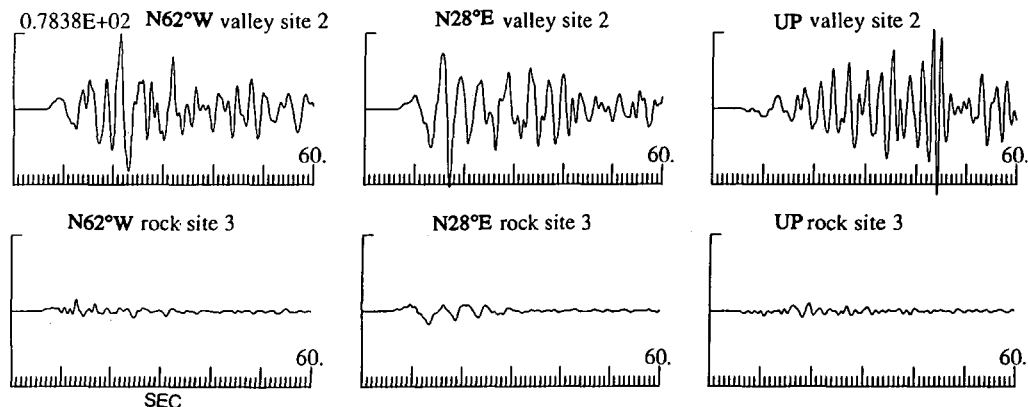


**FIGURE 6** Velocity synthetics at Sites 2 and 3 from 3-D simulation of M6.5 event (no anelastic attenuation). Note large amplitude difference between valley and rock sites. Synthetics plotted with the same scale.

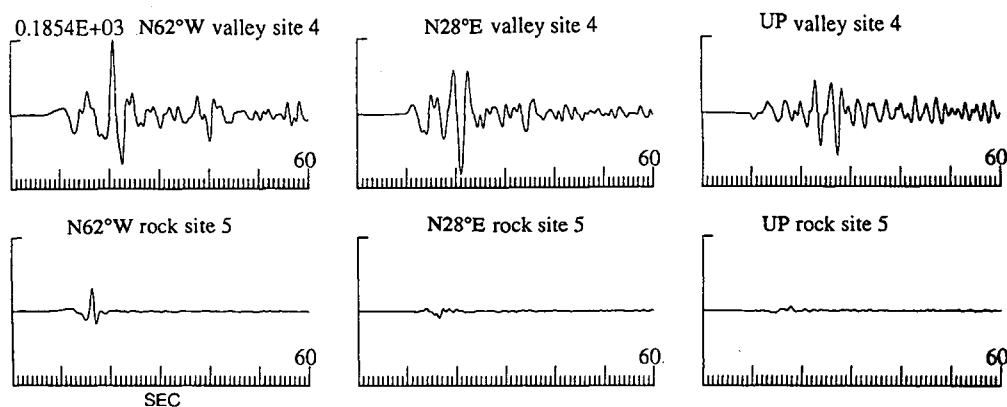


**FIGURE 7** Velocity synthetics at Sites 4 and 5 from 3-D simulation of M6.5 event (no anelastic attenuation). Site 4 has the largest horizontal ground motions in the simulation for this event. All synthetics are plotted with same scale. Peak amplitude is given in centimeters per second.

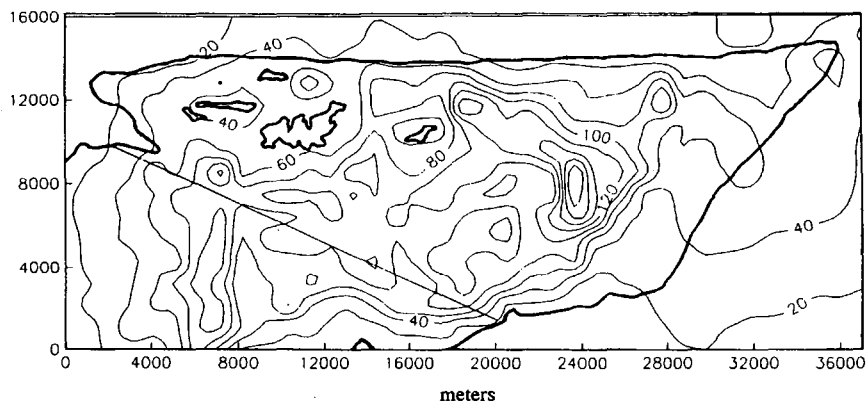


**FIGURE 8** Contour plot of peak horizontal motions from synthetics from 3-D simulations of M6.5 earthquake (southeast-propagating rupture). Values are from vector sum of both horizontal components and are given in centimeters per second (20-cm/sec contour interval). Peak motions are generally larger in the valley than in the surrounding rock. Largest motions are about 185 cm/sec. Thick lines denote edges of bedrock outcrops.

ration between the rock site (Site 1) and the valley sites (Sites 2 to 4). Love and Rayleigh waves are the largest phases in the synthetics for the basin sites. These surface waves are produced by conversion of the incident S-waves at the southern margin of the valley. Figure 12 compares the synthetic displacements (bottom row) with the observed motions for this aftershock recorded at Sunnysvale (top row). The agreement between the synthetics and data is good for the radial component. However, the Love waves on the transverse synthetic arrive earlier than the Love waves in the data. This may be due to overestimating velocities of the alluvium or underestimating the alluvium thickness. It is noteworthy that 1-D models would not even predict these large Love waves.

## SUMMARY

The 3-D simulations demonstrate the importance of S-wave-to-surface-wave conversions at the edges of the alluvial basin.

These surface waves often include the largest arrivals in the synthetic seismograms and greatly prolong the duration of shaking in the basin. The surface waves are reflected from the edges of the basin and travel in different directions across the valley. Large motions occur where the reflected waves constructively interfere with trapped waves behind the direct S-wave.

## FUTURE EFFORTS

The 3-D simulations represent a promising tool for predicting ground motions in sedimentary basins for frequencies  $\leq 1$  Hz. These efforts are largely limited by the lack of detailed knowledge of the velocity structure of sedimentary basins. For the two basins described above, the depth to bedrock is not known in most parts of the basins. The velocity and  $Q$  in the alluvium are poorly known. Refraction and reflection studies are needed to improve these models of the basin. The computational

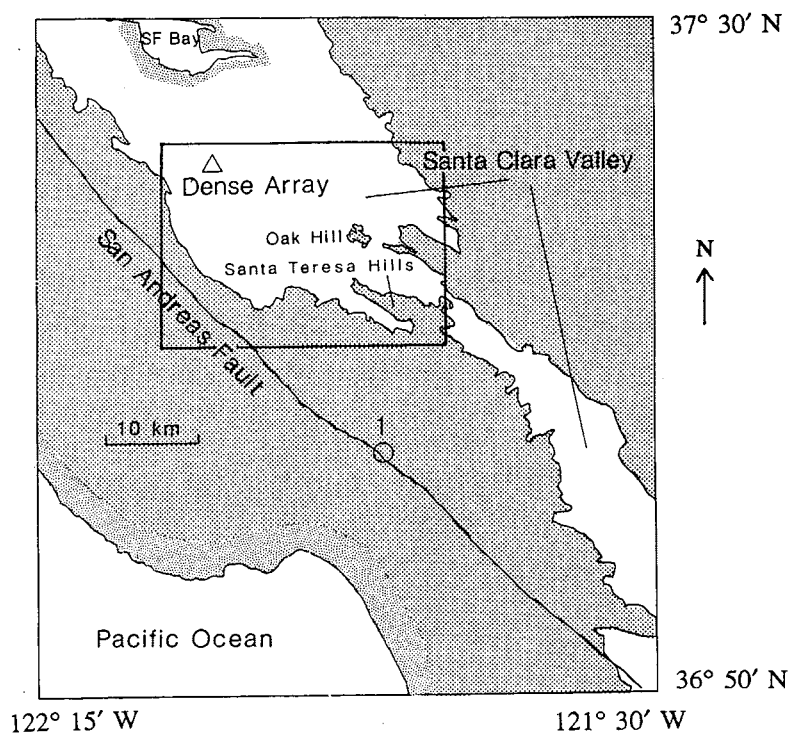


**FIGURE 9** Map of area south of San Francisco Bay. Box denotes area for Santa Clara Valley simulation. 1 is epicenter of  $M_L$  4.4 Loma Prieta aftershock (Oct. 25, 1989) that was modeled. Shaded areas are bedrock.

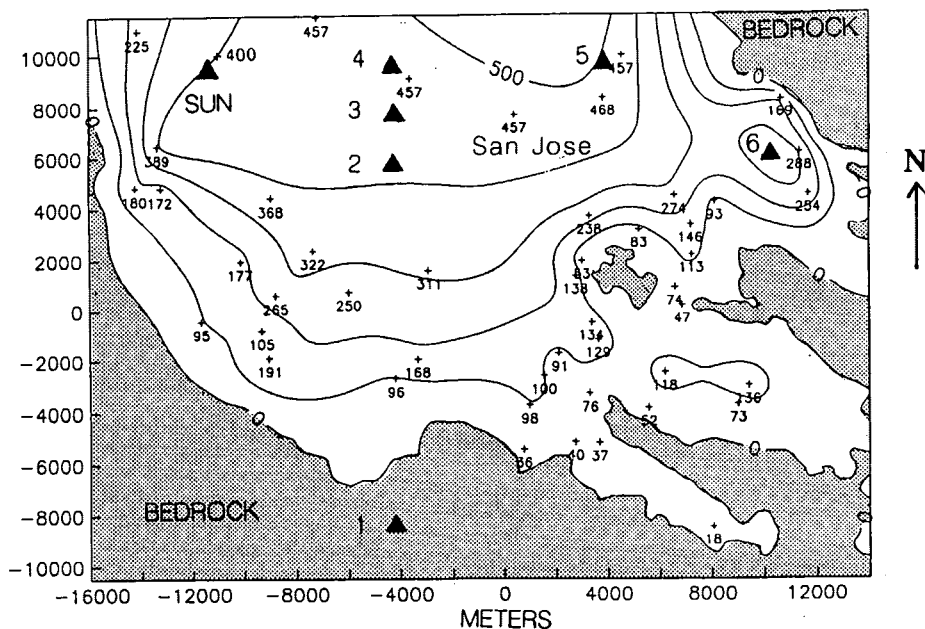


**FIGURE 10** Map of area used in Santa Clara Valley simulation. Crosses indicate depths to bedrock from water wells (in meters). Depths for crosses in center of valley are educated guesses, since water wells do not reach bedrock there. Contours show depth to bedrock for model used in simulation (100-m contour interval). The following values were used:  $V_S$  of 0.6 km/sec for alluvium, 2.0 km/sec for bedrock;  $V_P$  of 1.1 km/sec for alluvium, 3.5 km/sec for bedrock;  $\rho$  of 2.0 gm/cc for alluvium, 2.6 gm/cc for bedrock. Triangles show locations of receivers for synthetic seismograms. SUN denotes location of Sunnyvale dense array that recorded this Loma Prieta aftershock.

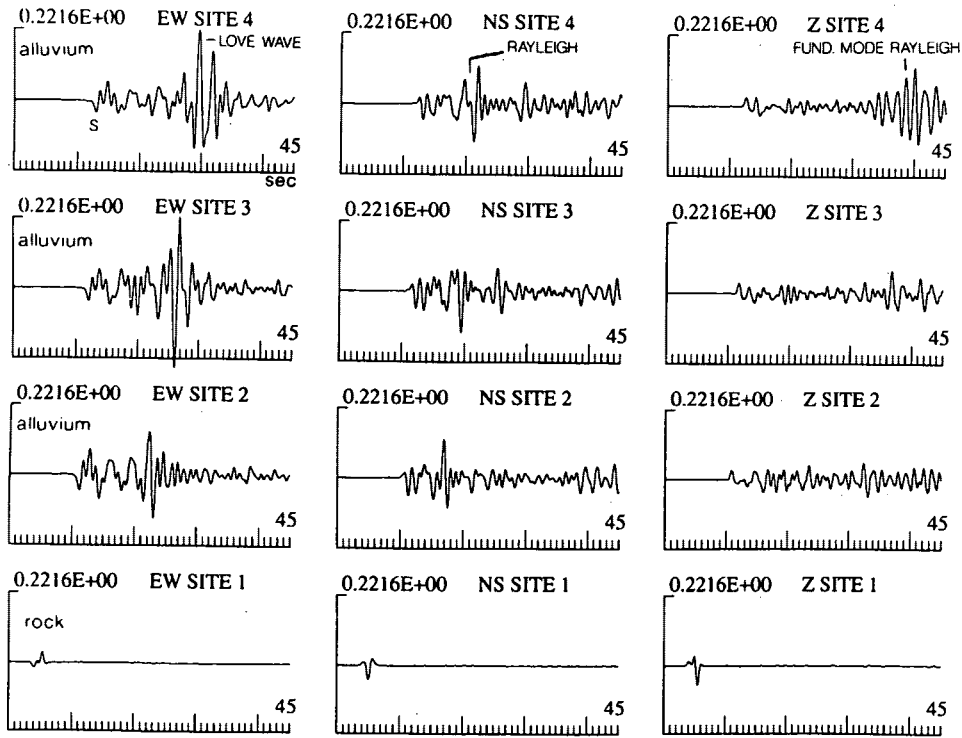


**FIGURE 11** Synthetic velocity seismograms from 3-D simulation for Santa Clara Valley (east-west, north-south, and vertical components). Peak velocities are shown above each panel in centimeters per second.

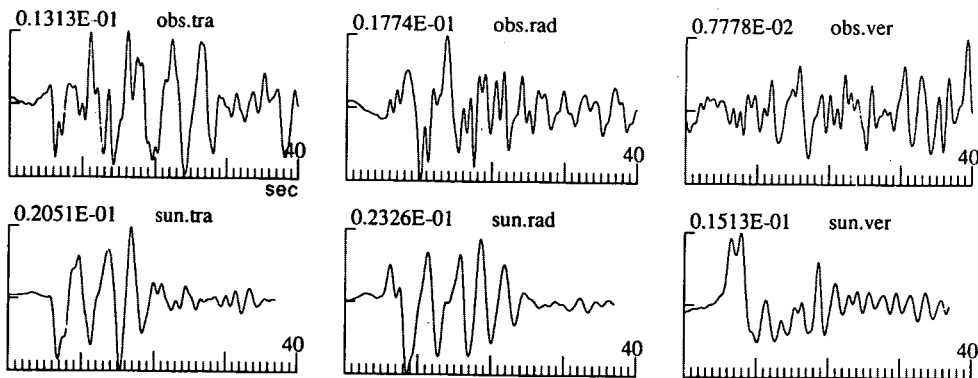


**FIGURE 12** Observed (*top*) and synthetic (*bottom*) ground displacements for the Sunnyvale dense array site. Transverse, radial, and vertical motions are shown. Peak amplitudes are given in centimeters. The synthetics were convolved with a time-varying  $Q$ -operator corresponding to a shear wave  $Q$  of 50 in the sediments.

techniques are now available to incorporate these details into the simulations, which require large amounts of supercomputer time. However, the 3-D calculations can also be done on fast workstations and are particularly suited to parallel processors. Accurate prediction of ground motions also requires consideration of a range of rupture scenarios, with varying rupture directivity and slip distribution.

## REFERENCES

1. Bard, P. Y., and M. Bouchon. The Seismic Response of Sediment-Filled Valleys. Part 1. The Case of Incident SH-waves. *Bulletin of the Seismological Society of America*, Vol. 70, 1980, pp. 1263-1286.
2. Vidale, J. E., and D. V. Helmberger. Elastic Finite-Difference Modeling of the 1971 San Fernando, California Earthquake. *Bul-*

- letin of the Seismological Society of America*, Vol. 78, 1988, pp. 122–141.
3. Frankel, A., S. Hough, P. Friberg, and R. Busby. Observations of Loma Prieta Aftershocks from a Dense Array in Sunnyvale, California. *Bulletin of the Seismological Society of America*, Vol. 81, 1991, pp. 1900–1922.
  4. Kawase, H., and K. Aki. A Study on the Response of a Soft Basin for Incident S, P, and Rayleigh Waves with Special Reference to the Long Duration Observed in Mexico City. *Bulletin of the Seismological Society of America*, Vol. 79, 1989, pp. 1361–1382.
  5. Phillips, W. S., S. Kinoshita, and H. Fujiwara. Basin-Induced Love Waves Observed Using the Strong Motion Array at Fuchu, Japan. *Bulletin of the Seismological Society of America*, Vol. 83, 1993, pp. 65–84.
  6. Spudich, P., and M. Iida. The Seismic Coda, Site Effects, and Scattering in Alluvial Basins Studied Using Aftershocks of the 1986 North Palm Springs, California Earthquake as Source Arrays. *Bulletin of the Seismological Society of America*, Vol. 83, 1993, in press.
  7. Frankel, A., and J. Vidale. Three-Dimensional Simulations of Seismic Waves in the Santa Clara Valley, California, from a Loma Prieta Aftershock. *Bulletin of the Seismological Society of America*, Vol. 82, 1992, pp. 2045–2074.
  8. Frankel, A. Three-Dimensional Simulations of Ground Motions in the San Bernardino Valley, California, for Hypothetical Earthquakes on the San Andreas Fault. *Bulletin of the Seismological Society of America*, Vol. 83, 1993, in press.
- 
- Any use of a product name in this paper is for descriptive purposes only and does not constitute endorsement by the U.S. government.*
- Publication of this paper sponsored by Committee on Engineering Geology.*